Supporting Information

The biobehavior, biocompatibility and theranostic application of SPNS and Pd@Au nanoplates in rats and rabbits

Contents:

Figure S12: Cellular uptake of SPNS and Pd@Au by VX2 cells.

Figure S13: PTT efficiency for *in vitro* killing VX2 cells.

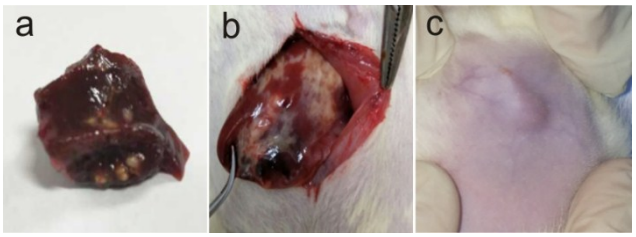

Figure S1: The photos of (a) rabbit orthotopic liver tumor, (b) rats orthotopic liver tumor and (c) subcutaneous tumor.

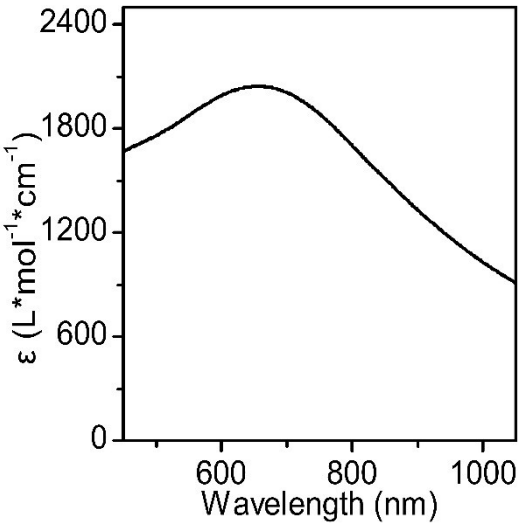

Figure S2: The molar absorption coefficients of SPNS at different wavelengths (Concentration of SPNS: 40 ppm).

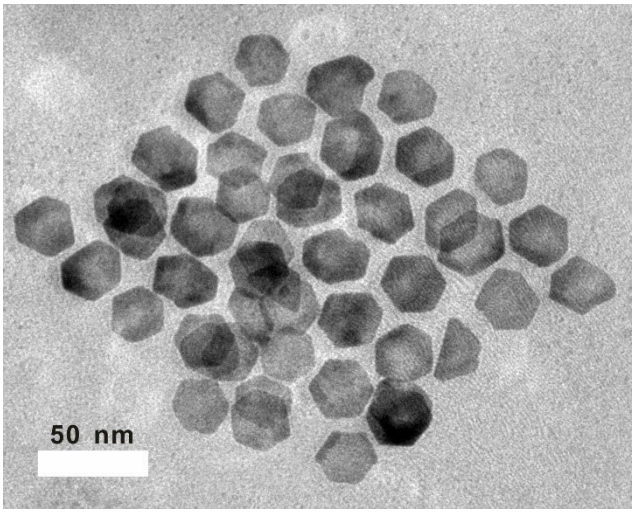

Figure S3: The TEM image of Pd@Au-PEG.

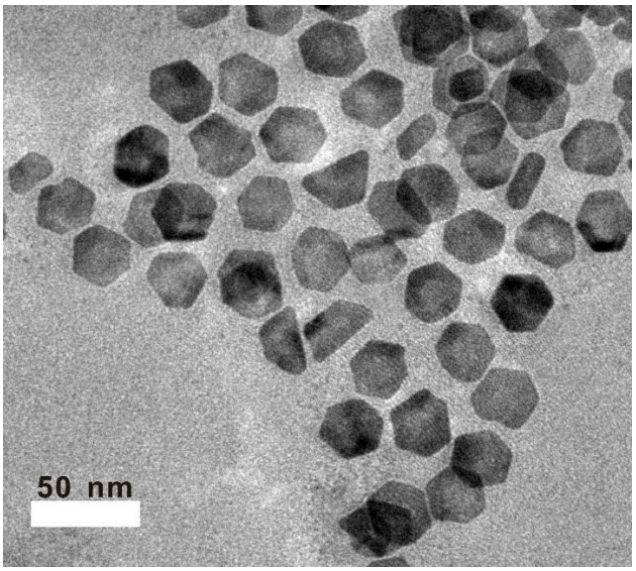

Figure S4: The TEM image of Pd@Au-PEG after laser irradiation (0.5 W/cm^2, 10 min).

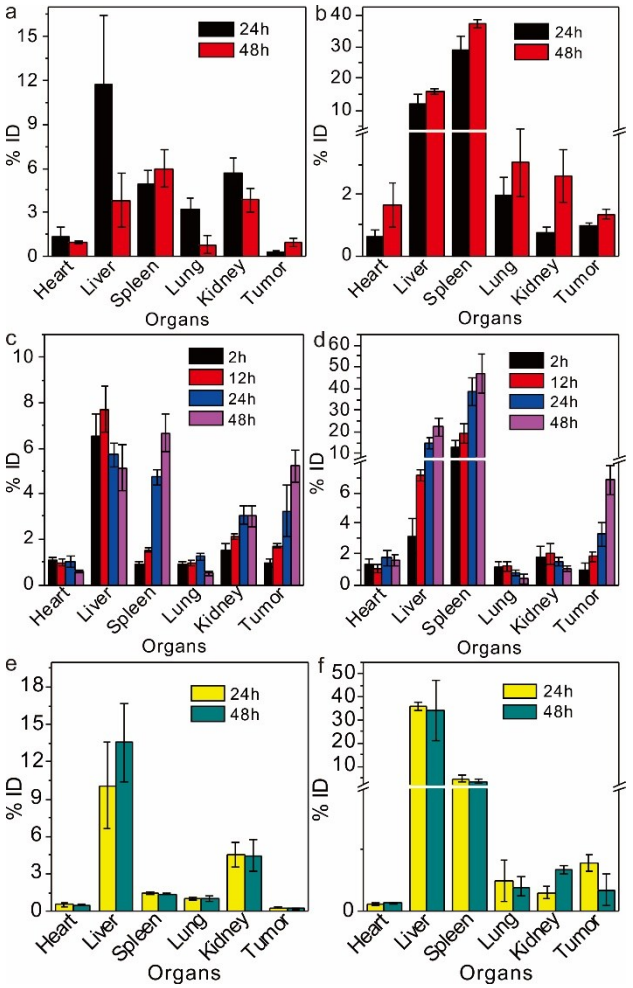

Figure S5: The biodistribution of SPNS and Pd@Au calculated in % ID. (a) SPNS and (b) Pd@Au in orthotopic liver tumor-bearing rats; (c) SPNS and (d) Pd@Au in subcutaneous tumor-bearing rats; (e) SPNS and (f) Pd@Au in orthotopic liver tumor-bearing rabbits.

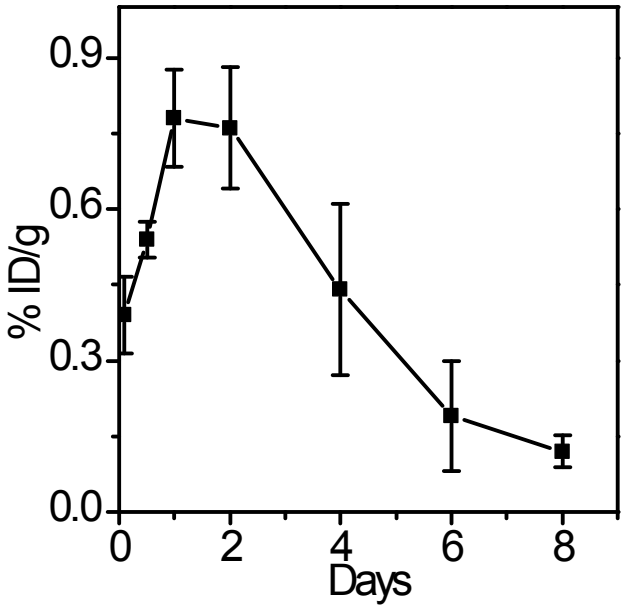

Figure S6: The accumulation amount changes of SPNS in rats' kidney.

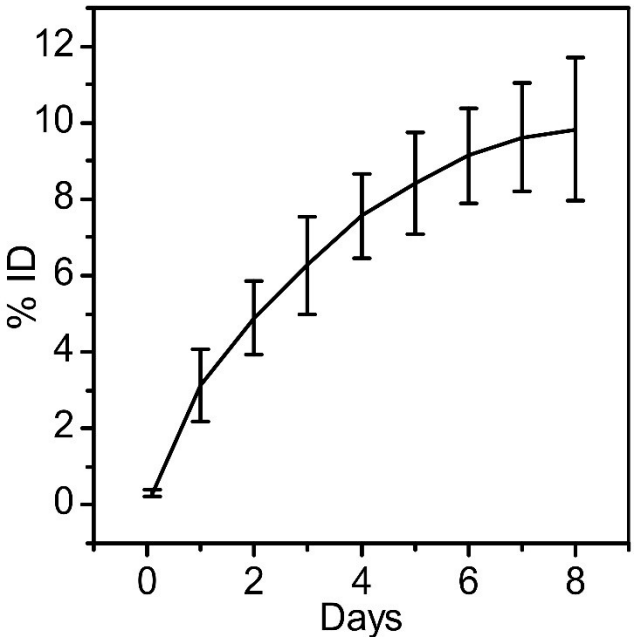

Figure S7: The excretion of Pd@Au by feces.

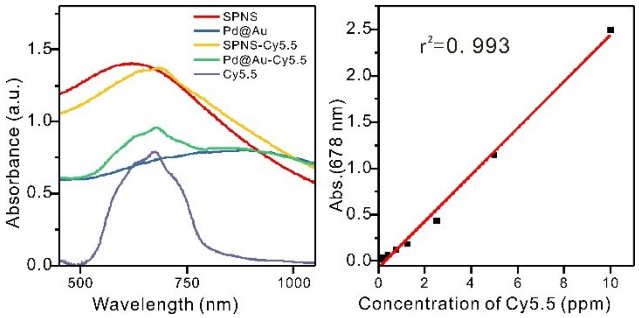

Figure S8: The loading efficiencies of Cy5.5 on SPNS and Pd@Au. (a) UV-Vis-NIR absorption spectra of SPNS, SPNS-Cy5.5, Pd@Au, Pd@Au-Cy5.5 and Cy5.5. (b) The standard absorption curve of Cy5.5 at 678 nm.

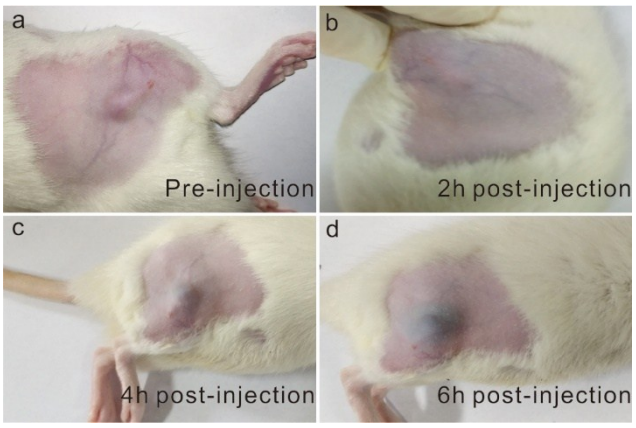

Figure S9: The color changes of rat subcutaneous tumors after intravenous injection of SPNS-PEG.

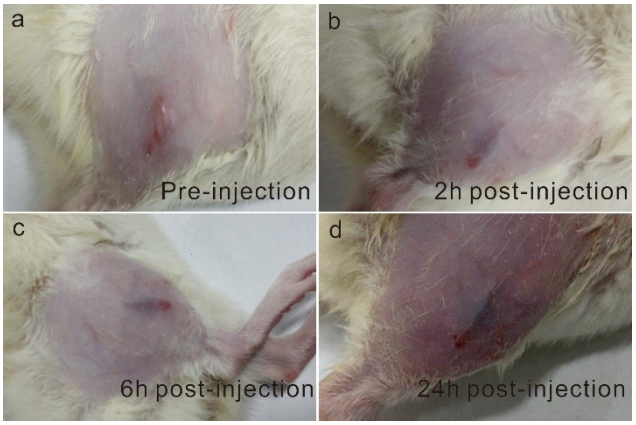

Figure S10: The color changes of rat subcutaneous tumors after intravenous injection of Pd@Au-PEG.

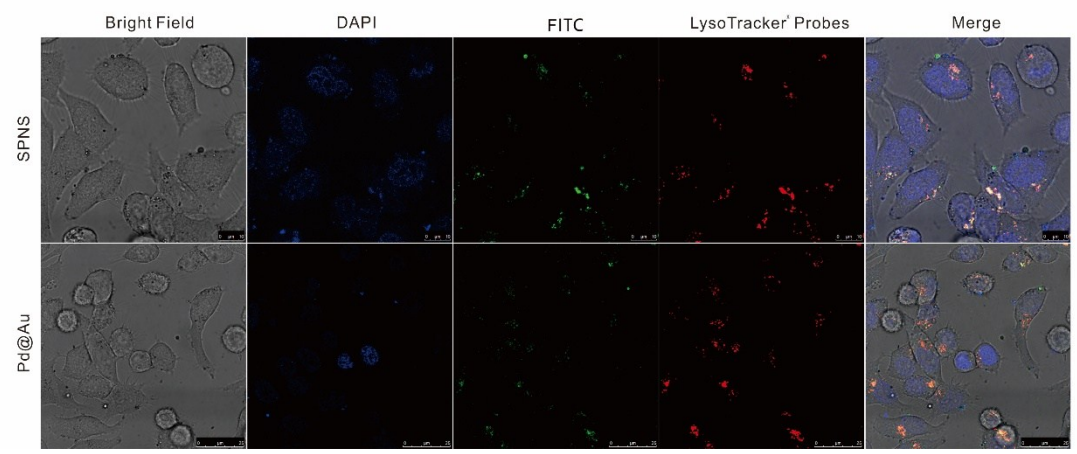

Figure S11: Cellular uptake of SPNS and Pd@Au by W256 cells.

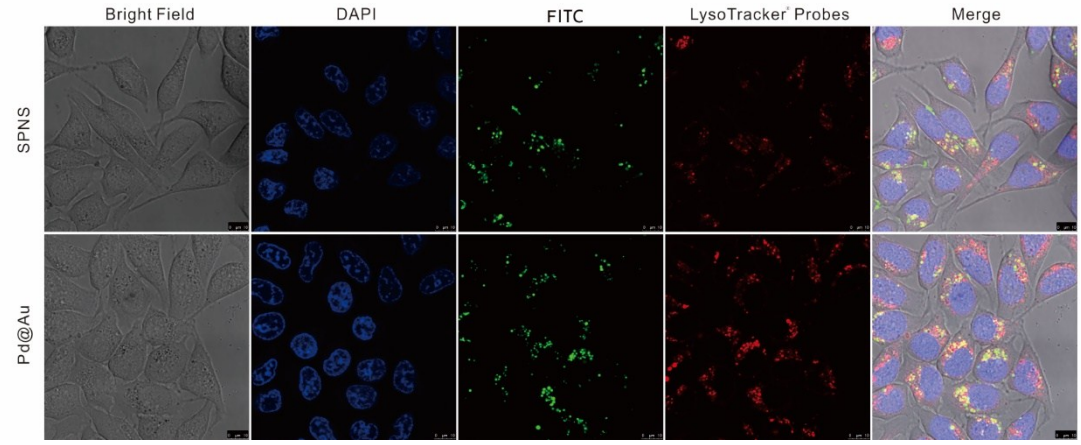

Figure S12: Cellular uptake of SPNS and Pd@Au by VX2 cells.

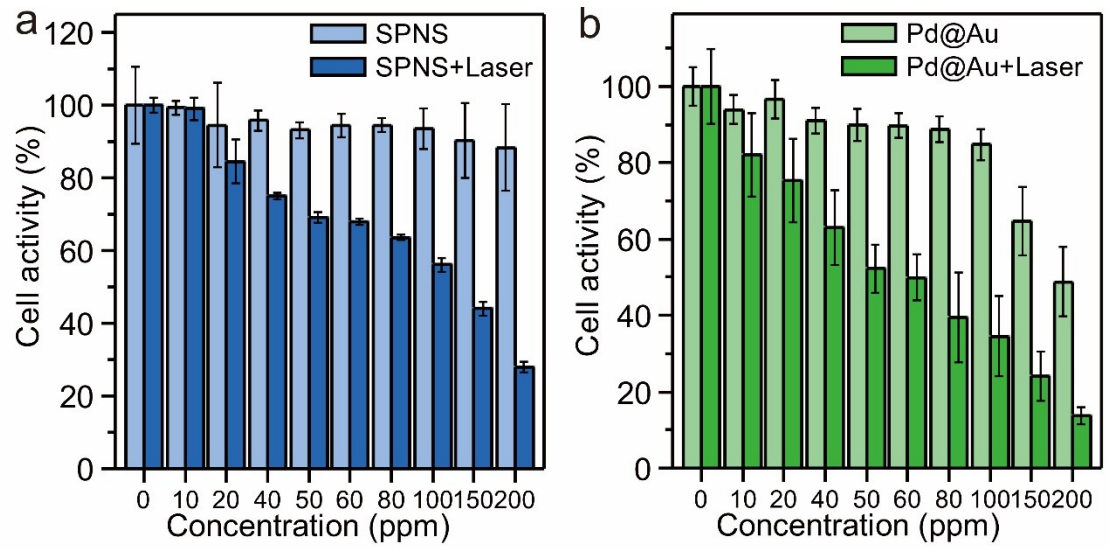

Figure S13: PTT efficiency of (a) SPNS and (b) Pd@Au for *in vitro* killing VX2 cells.